J Solid State Electrochem (2012) 16:811–818
DOI 10.1007/s10008-011-1433-5

ORIGINAL PAPER

Effect of synthesis temperature and molar ratio of organic lithium salts on the properties and electrochemical performance of $LiFePO_4$/C composites

Zhongqi Shi · Ming Huang · Kerun Yang · Xuebu Hu · Bin Tan · Xinglan Huang · Zhenghua Deng

Received: 27 February 2011 / Revised: 5 May 2011 / Accepted: 8 May 2011 / Published online: 31 May 2011

Abstract $LiFePO_4$/C cathode materials were synthesized through in situ solid-state reaction route using Fe_2O_3, $NH_4H_2PO_4$, $Li_2C_2O_4$, and lithium polyacrylate as raw materials. The precursor of $LiFePO_4$/C was investigated by thermogravimetric/differential thermal analysis. The effects of synthesis temperature and molar ratio of organic lithium salts on the performance of samples were characterized by X-ray diffraction, scanning electron microscopy, electrochemical impedance spectra, cyclic voltammogram, and constant current charge/discharge test. The sample prepared at optimized conditions of synthesis temperature at 700 °C and molar ratio with 1.17:1 exhibits excellent rate performance and cycling stability at room temperature.

Keywords $LiFePO_4$/C · Synthesis temperature · Organic lithium salt · Lithium-ion batteries

Z. Shi · M. Huang · K. Yang · B. Tan · X. Huang · Z. Deng (✉)
Chengdu Institute of Organic Chemistry,
Chinese Academy of Sciences,
Chengdu, Sichuan 610041, People's Republic of China
e-mail: zhdeng@cioc.ac.cn

Z. Shi · M. Huang · K. Yang · B. Tan · X. Huang · Z. Deng
Graduate School of Chinese Academy of Sciences,
Beijing 100039, People's Republic of China

X. Hu
Department of Chemistry and Materials,
Sichuan Normal University,
Chengdu, Sichuan 610068, People's Republic of China

X. Hu · Z. Deng
Zhongke Laifang Power Science & Technology Co., Ltd,
Chengdu, Sichuan 610041, People's Republic of China

Introduction

Olivine-type $LiFePO_4$ [1] is becoming the most promising cathode material of green lithium-ion batteries for the applications in electric vehicle and hybrid electric vehicle owning to its particular advantages with regard to low cost, nontoxicity, high theoretical capacity(170 mAh g^{-1}), thermal stability at rather high temperature, and high safety. However, $LiFePO_4$ suffers from some obstacles, such as poor electronic conductivity and Li-ion diffusion coefficient, which result in initial capacity loss and poor rate performance. To overcome the problems, several methods have been developed, such as coating electronically conductive additives [2] or doping with supervalent cation [3] to enhance the electronic conductivity and minimizing the particle size [4] to reduce the Li-ion and electron diffusion distance.

Synthesis temperature is one of the most important factors of solid-state reaction, which is considered as the appropriate method for producing commercial $LiFePO_4$. Related researches [5–8] have shown that synthesis temperature has an obvious effect on the particle size, crystallinity, and even the electrochemical performance of the $LiFePO_4$. However, different raw materials and methods result in the diversity of the optimized synthesis temperature, which is ranging from 500 °C to 900 °C. It is common that inorganic lithium salt [9–11] and carbonaceous compound [12–15] are used as lithium source and carbon source, respectively. In our present work, the mixture of $Li_2C_2O_4$ and lithium polyacrylate (PAALi) cannot only be used as lithium source but also be used as carbon source. Moreover, carboxylic acid free radicals obtained from the pyrolysis of $Li_2C_2O_4$ and PAALi can reduce ferric iron to divalent iron by a sequence of free-radical reactions [16,

17]. It has been confirmed in our previous paper [18] that olivine-type $LiFePO_4$ can also be obtained from Fe_2O_3 by the reducibility of carboxylic acid free radicals from $Li_2C_2O_4$ under inert atmosphere, without adding any carbon source. Via varying the mixture mole ratio of $Li_2C_2O_4$ to PAALi, we can control the carbon content, which also has a significant effect on the performance of the $LiFePO_4$.

In this paper, we research the effect of synthesis temperature and molar ratio of organic lithium salts in order to achieve $LiFePO_4$/C composites with excellent electrochemical performances.

Experimental

$LiFePO_4$/C was synthesized by preheating at 450 °C for 2 h and held at 500 °C, 600 °C, 700 °C, 800 °C, 850 °C for 10 h, respectively, in an N_2 atmosphere, with the starting materials of Fe_2O_3, $NH_4H_2PO_4$, $Li_2C_2O_4$, and PAALi. PAALi was obtained via dissolving a stoichiometric amount of $LiOH{\cdot}H_2O$ into an aqueous solution of polyacrylic acid (PAA). The samples were labeled as S500, S600, S700, S800, and S850, respectively. Ensuring the molar ratio of $Li/Fe/PO_4$=1:1:1, the two lithium sources, $Li_2C_2O_4$ and PAALi with different mixture mole ratios (2.83:1, 1.72:1, 1.17:1, 0.83:1, 0.68:1, respectively), were ball-milled with other starting materials and then were preheated at 450 °C for 2 h and held at 700 °C for 10 h. And all the samples also were labeled as H1, H2, H3, H4, and H5, respectively. All the precursors are obtained by wet ball milling with a medium of water.

Thermogravimetric–differential thermal analysis (TG–DTA) measurements have been performed (NETZSCH STA 409 PC/PG) from 20 °C to 850 °C at a heating rate of 10 °C min^{-1} under argon atmosphere. The crystalline

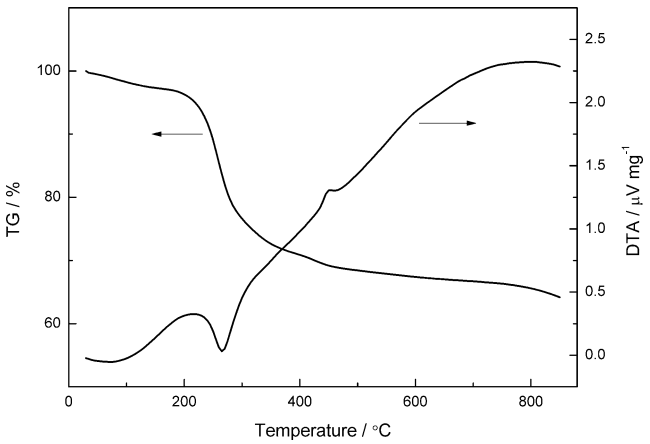

Fig. 1 TG–DTA curves of the $LiFePO_4$/C precursor recorded from 20 °C to 850 °C with a heating rate of 10 °C min^{-1} under an argon flow of 30 mL min^{-1}

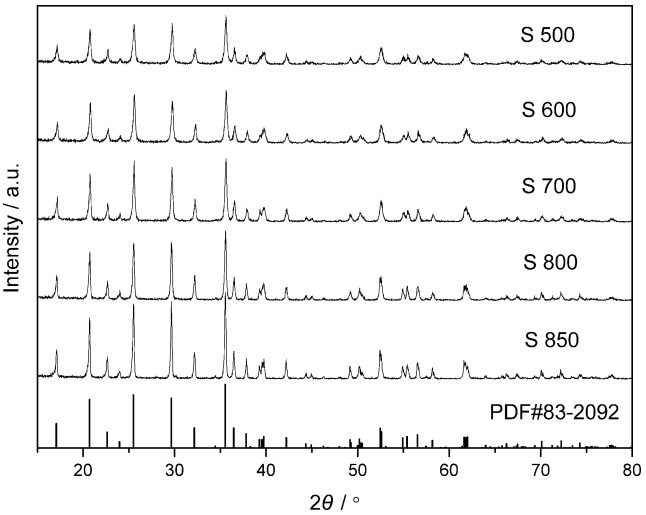

Fig. 2 XRD patterns of the $LiFePO_4$/C composites synthesized at different temperatures

phase of the sample was identified by X-ray diffraction (XRD) analysis using Cu Kα radiation with a step of 0.02° (X'Pert Pro MPD, Philip). The morphology of powder was observed by scanning electronic microscope (SEM; Inspect F, FEI). The carbon content of samples was determined by an elemental analyzer (Carlo Erba 1106, Carlo Erba).

The cathodes were prepared via mixing 90 wt.% $LiFePO_4$/C composite, 5 wt.% conductive carbon black (Super P, TIMCAL), and 5 wt.% aqueous binder LA132 (from Indigo, China) in distilled water. The resultant slurry was then coated onto an aluminum foil. The coated aluminum foil was dried for 10 h in a vacuum oven at 100 °C and then punched into circular disks with active material loading of about 4 to 5 mg cm^{-2}.

The lithium foil was used as the counter electrode, and 1 M $LiPF_6$ in EC/DEC/EMC=1:1:1 was used as the electrolyte. The 2032-type coin cells were assembled in an argon-filled glove box. The charged/discharged test was performed at various C rates in the voltage range of 2.5–4.3 V (versus Li/Li^+) at ambient temperature. Electrochemical impedance spectra (EIS) were investigated by a Solartron SI 1260/1287(UK) impedance analyzer in the frequency range of 10^{-1}–10^6 Hz. Cyclic voltammetry (CV) tests were carried out in the voltage range of 2.5–

Table 1 The lattice parameters and calculated crystallite size of the $LiFePO_4$/C composites synthesized at different temperatures

Sample	*a* (Å)	*b* (Å)	*c* (Å)	*V* (Å^3)	*D* (nm)
S500	10.33256	6.00967	4.69161	291.33	34
S600	10.32476	6.01144	4.68591	290.84	36
S700	10.33044	6.01221	4.69361	291.51	40
S800	10.34119	6.01694	4.69850	292.35	44
S850	10.34388	6.01795	4.70255	292.73	55

4.3 V at a scan rate of 0.1 mV s^{-1} (Arbin-001 MITS Pro 3.0-BT2000, Arbin).

Results and discussion

Thermal analysis

Figure 1 shows the TG/DTA curves for the precursor of $LiFePO_4$/C from room temperature to 850 °C with a heating rate of 10 °C min^{-1} in an argon flow rate of 30 mL min^{-1}. The endothermic peak at around 85.3 °C and small mass loss corresponded to the volatilization of absorption water of the precursor. Another endothermic peak at around 265.3 °C and a continuous mass loss can be related to the thermal decomposition of the partial reactants. A solely petite exothermic peak at 452.2 °C was observed in the DTA curve, but no appreciable mass loss is observed from 450 °C to 850 °C, indicating that the crystallization of $LiFePO_4$ takes place in this temperature and the reaction was

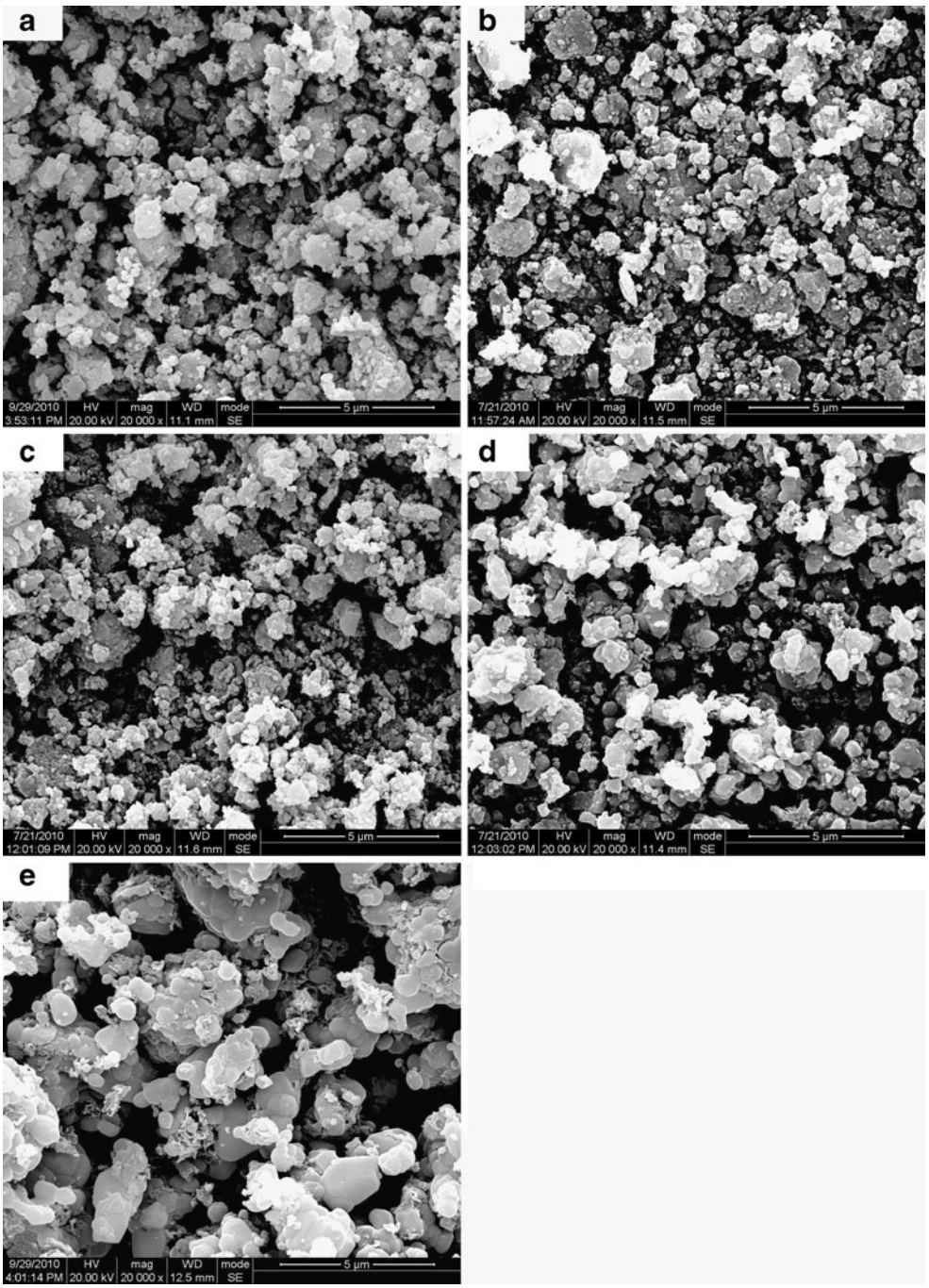

Fig. 3 SEM images of the $LiFePO_4$/C composites synthesized at different temperatures of 500 °C (**a**), 600 °C (**b**), 700 °C (**c**), 800 °C (**d**), and 850 °C (**e**)

complete. Therefore, to obtain a single-phase olivine-type $LiFePO_4$, the precursor was preheated at 450 °C and finally held at temperature ranging from 500 °C to 850 °C for 10 h.

Physical and electrochemical properties of $LiFePO_4$/C composite with different synthesis temperatures

Figure 2 shows the X-ray diffraction patterns of the $LiFePO_4$/C composites synthesized at 500 °C, 600 °C, 700 °C, 800 °C, and 850 °C for 10 h, respectively. All the patterns reveal a single-phase olivine $LiFePO_4$, indexing to the JCPDS no. 83-2092. It is out of accordance with experiments of Kim et al. [6] and Wang et al. [5] that no impurities were observed in our $LiFePO_4$/C composites synthesized at varied temperatures. It indicates that the carboxylic acid free-radical reactions of our system can effectively inhibit the production of the impurities, such as Fe_2O_3, Li_3PO_4, etc. Moreover, it is obvious that the diffraction peaks get sharper and more intense with increasing the synthesis temperature from 500 °C to 850 °C because of the improvement of the crystallinity. Table 1 lists the lattice parameters and the calculated crystallite size based on D_{311}, D_{211}, and D_{111} for the five samples. We can find that the lattice parameters of five samples have almost the same values. However, with the increasing of the synthesis temperature, the crystallite size D rises from 34 nm at 500 °C to 55 nm at 850 °C. It is believed that crystallite size may be increased as increasing the synthesis temperature because of the improvement of the crystallinity.

Figure 3 shows the SEM images of the $LiFePO_4$/C composites synthesized at the temperatures ranging from 500 °C to 850 °C. With the temperature increasing, the particle size significantly increase and the morphologies become more non-homogeneous. The average particle size remains in the range of 100–300 nm at 500–700 °C, but the size grows to 0.4–2 μm at 800–850 °C. The increased particle size may increase the Li-ion diffusion distance and then inhibit the electrochemical performance of $LiFePO_4$/C composite.

Table 2 Carbon contents of the samples synthesized from $Li_2C_2O_4$ and PAALi with different mixture mole ratios

Sample	$Li_2C_2O_4$/PAALi (mole ratio)	Carbon content (%)
H1	2.83:1	1.72
H2	1.72:1	2.69
H3	1.17:1	3.76
H4	0.83:1	4.84
H5	0.68:1	5.86

Figure 4 presents the special discharge capacities of the samples synthesized at different temperatures with the number of cycles at 0.2 C rate. With increasing the temperature from 500 °C to 700 °C, the initial discharge capacity gradually increases from 100.15 to 145.68 mAh g^{-1} because of the improvement of the crystallinity. However, as further increasing the temperature, the initial capacities significantly reduce to 122.58 and 102.81 mAh g^{-1} at 800 °C and 850 °C, respectively. It is mainly due to the growth and non-homogeneity of the particle size. After 10 cycles, all the samples exhibit great cycling performances except sample S800 and sample S850. Therefore, the optimal sample synthesized at 700 °C exhibits the highest discharge capacity and most best cycling behavior.

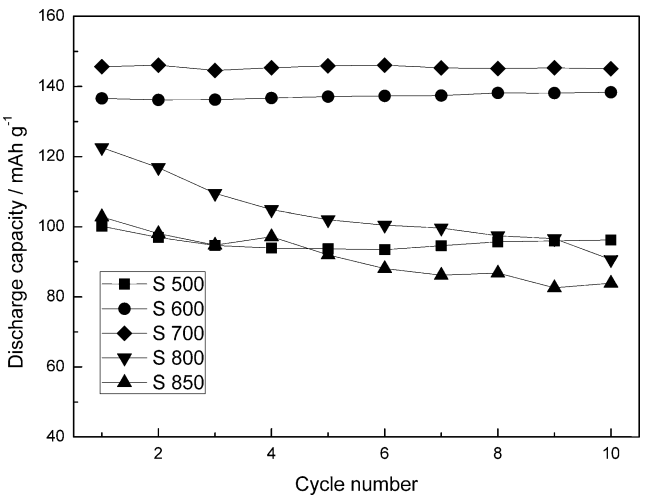

Fig. 4 Cycle performances of the $LiFePO_4$/C composites synthesized at different temperatures

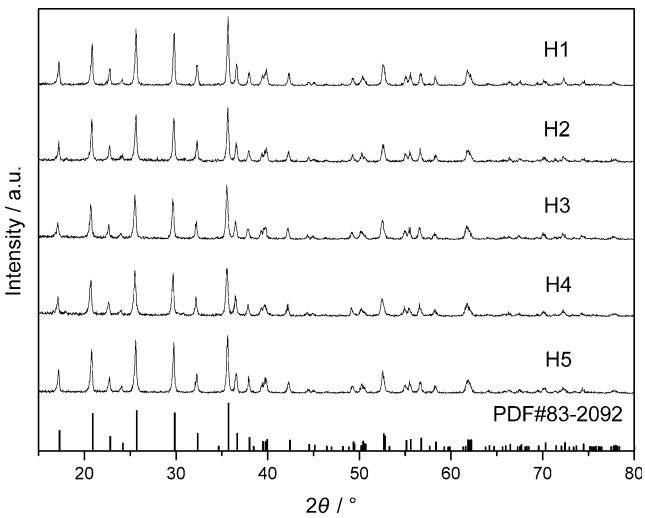

Fig. 5 XRD patterns of the $LiFePO_4$/C composites synthesized from $Li_2C_2O_4$ and PAALi with different mixture mole ratios of 2.83:1 (H1), 1.72:1 (H2), 1.17:1 (H3), 0.83:1 (H4), and 0.68:1 (H5)

Physical and electrochemical properties of $LiFePO_4$/C composite with different mixture mole ratios of $Li_2C_2O_4$ to PAALi

The effect of the mixture mole ratio of $Li_2C_2O_4$ to PAALi on the properties and electrochemical performance of $LiFePO_4$/C composites is researched in this section. Table 2 lists the carbon contents of the samples by the elemental analyzer. It shows that carbon content increases as decreasing the mole ratio. The conductive carbon cannot only reduce the particle size but also improve the electronic conductivity of $LiFePO_4$, but at the cost of reducing the tap density of the material. Therefore, it is essential to optimize the carbon content in order to achieve the best performance. Figure 5 shows the X-ray diffraction patterns of the $LiFePO_4$/C composites synthesized with different mixture mole ratios of $Li_2C_2O_4$ to PAALi. The diffraction patterns of all the samples are well matched with the standard pattern of $LiFePO_4$ with an orthorhombic *Pmnb* (JCPDS no. 83-2092). The results reveal that pure $LiFePO_4$ would

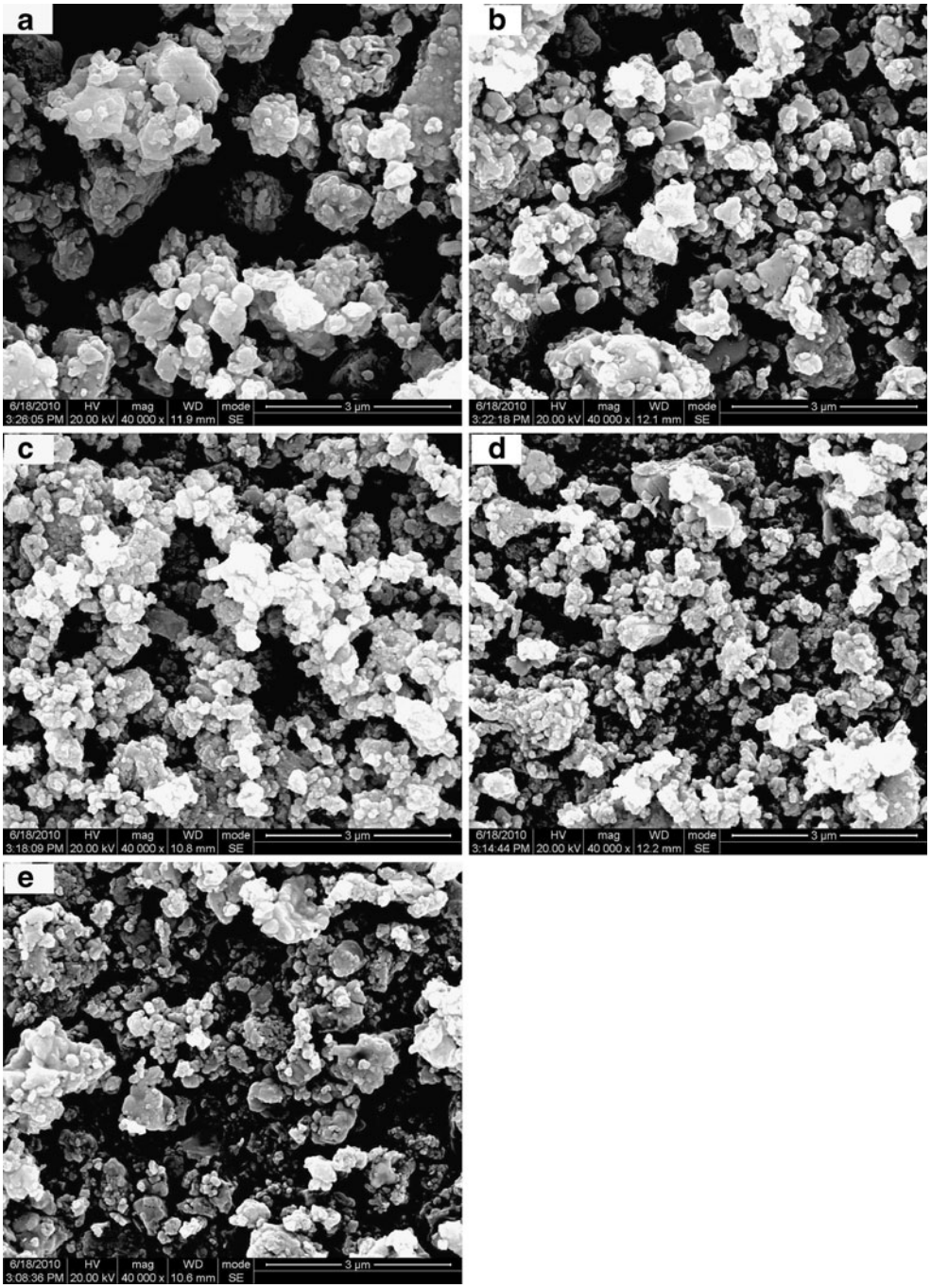

Fig. 6 SEM images of the $LiFePO_4$/C composites synthesized from $Li_2C_2O_4$ and PAALi with different mixture mole ratios of 2.83:1 (**a**), 1.72:1 (**b**), 1.17:1 (**c**), 0.83:1 (**d**), and 0.68:1 (**e**)

be suitable synthesized whatever the mole ratio (carbon content) is because no impurity phases were detected. However, the intensity of the diffraction peaks gradually decreases with the growth of the carbon contents. It is due to that the carbon can effectively inhibit the growth of the crystalline grain size. The particle morphologies of the samples can be seen in Fig. 6. The particle sizes of all samples are less than 1 μm. It indicates that the pyrolytic carbon from PAALi plays an important role in controlling the particle growth of $LiFePO_4$. We can also find that the smaller particles are obtained with increasing the mole ratio. Thus, the diminution of the particle size is mainly related to the increasing carbon content, which may affect the electrochemical performance of $LiFePO_4$ cathode.

Figure 7 presents the Nyquist plots of the samples with different carbon contents. All the impedance spectra have a semicircle and a linear spike in the high-frequency and low-frequency regions, respectively. The semicircle refers to the charge-transfer resistance of electrochemical reaction, while the linear spike refers to the thin-layer ionic diffusion-controlled Warburg impedance [19, 20]. The charge-transfer resistance R_{ct} of sample H1, H2, H3, H4, and H5 are nearly 813, 505, 263, 293, and 385 Ω, respectively. It is noted that the R_{ct} of sample H3 presents the minimum with the appropriate carbon content. It is believed that the conductive carbon uniformly dispersed among the $LiFePO_4$ particles can form a good electronic conduction path and effectively improve the conductivity. Thus, the increasing carbon content can lead to the improvement of conductivity, which is beneficial to the kinetic behaviors during charge and discharge process. However, as further increasing the carbon content, the conductivity reduces gradually, which may due to the suppressions of electron transfer and Li-ion diffusion by the excessive carbon. It can be expected that low residence gives small electrode polarization.

Cyclic voltammogram profiles of the samples are shown in Fig. 8. Similarly, each of the five samples displays a good reversibility and has only one anodic peak and one cathodic peak, which correspond to the two-phase charge/discharge reaction of the Fe^{2+}/Fe^{3+} redox couple. Dissimilarly, the position of the redox peak of five samples is different from each other because of the different carbon contents. The voltage intervals (ΔV) between the anodic peak and cathodic peak of samples H1, H2, H3, H4, and H5 are 0.50, 0.43, 0.38, 0.54, and 0.55 V, respectively. It can be found that insufficient or excessive carbon (mole ratio of $Li_2C_2O_4$ to PAALi is too large or too small) will all lead to the increase of the voltage interval, which is closely associated with the electrode polarization. With the appropriate carbon content, sample H3 has the smallest electrode polarization, which implies the great electrochemical performance.

The initial discharge curves of the five samples at 0.2 C rate are shown in Fig. 9. It can be found that all samples show a smooth discharge plateau at around 3.4 V which corresponds to the pure $LiFePO_4$. Among these samples, sample H3 shows the largest initial discharge capacity of 156.37 mAh g^{-1}, about 92% of the theoretical capacity, which can be due to the highest conductivity and smallest electrode polarization. The result is greatly in accord with the analysis by EIS and CV. The increase of discharge capacity as increasing the carbon content is mainly due to that the conductive carbon enhances the electron conduction and reduces the electrode polarization. However, excessively increasing carbon content may suppress the electron transfer and Li-ion diffusion in the carbon layer and then inhibit the discharge capacity unfortunately. Figure 10

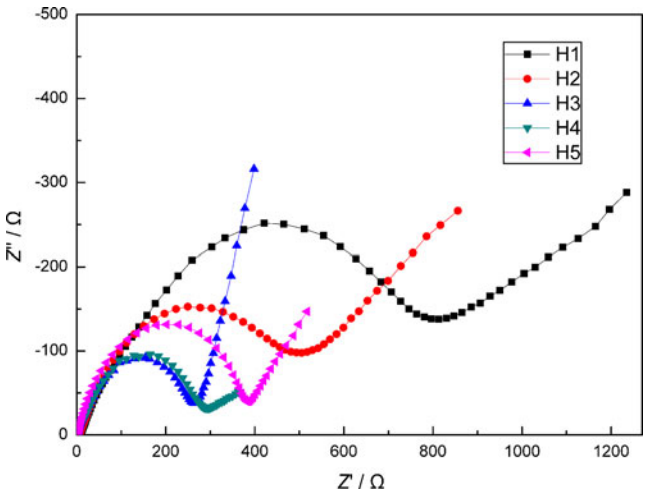

Fig. 7 Nyquist plots of $LiFePO_4$/C composites with different carbon contents at the frequency range of 10^{-1}–10^6 Hz

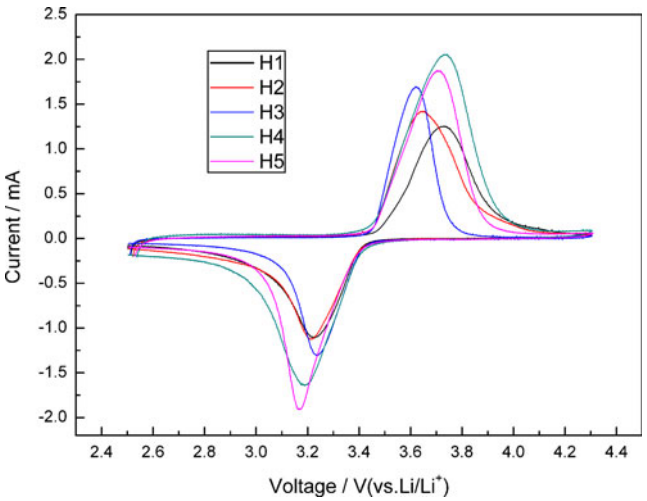

Fig. 8 CV profiles of the $LiFePO_4$/C samples with different carbon contents in the voltage range of 2.5–4.3 V at a scan rate of 0.1 mV s^{-1}

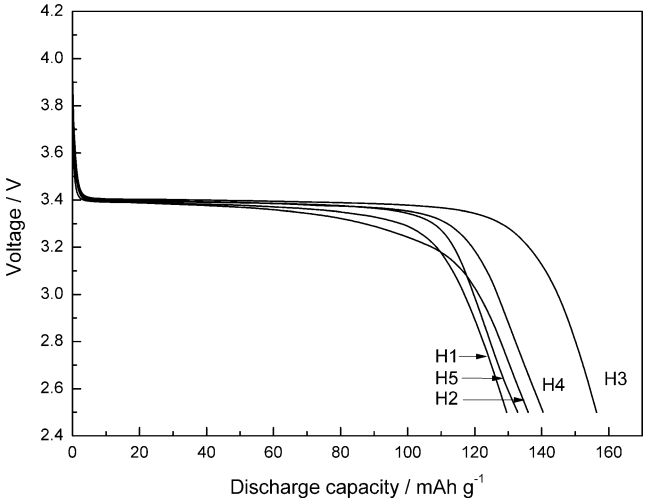

Fig. 9 Initial discharge curves of the $LiFePO_4$/C composites with different carbon contents at 0.2 C between 2.5 and 4.3 V

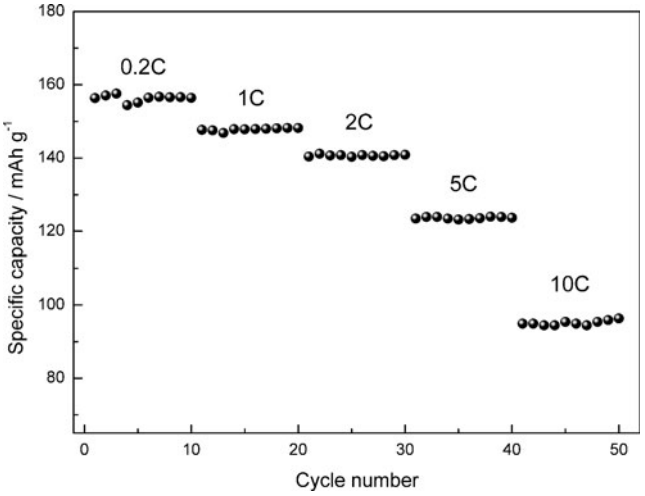

Fig. 11 Rate performance of the $LiFePO_4$/C composite derived from optimized synthesis conditions

shows the cycle performance of the five samples at 0.2 C rate. After 20 cycles, the discharge capacity of sample H1 reduces rapidly from 129.55 to 116.65 mAh g^{-1} with 9.96% capacity fading, showing the poorest cycle performance. We attribute the largest fading to the non-homogeneous carbon distribution, the largest particle size, and the biggest electrode polarization. It is noted that the cycle performance becomes better with the increasing carbon content. The capacity fading of H3 with 3.76% carbon content is only 0.20% because of the improvement of conductivity. From the above discussions, it can be concluded that the optimal mixture mole ratio of $Li_2C_2O_4$ to PAALi is 1.17:1.

The rate and cycling performance of the optimized sample

With the optimal synthesis temperature of 700 °C and optimal mixture mole ratio of 1.17:1, we synthesize the best sample and investigate the rate performance of it, as shown in Fig. 11. Although the discharge capacities are decreased with increasing the discharge rates, they are well retained at varied rates during several cycles. Even at high rates of 5 and 10 C, the discharge capacity still remains 123.44 and 94.93 mAh g^{-1}, respectively, because of the improvement of the conductivity. Figure 12 shows the cycling performance of the optimized sample at 5 and 10 C. The sample exhibits great stability that the discharge capacity fading of it are only 0.76% at 5 C after 50 cycles and 0.99% at 10 C after 80 cycles.

Conclusions

In order to optimize the synthesis conditions and obtain the best performance of $LiFePO_4$, the effects of synthesis

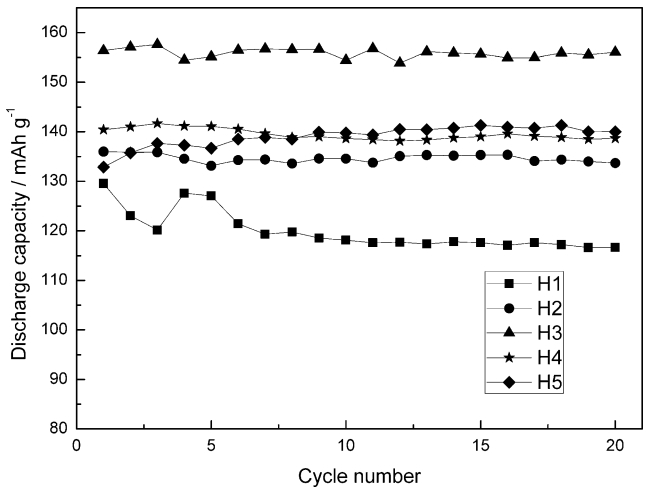

Fig. 10 Cycle performances of the $LiFePO_4$/C composites with different carbon contents at 0.2 C rate

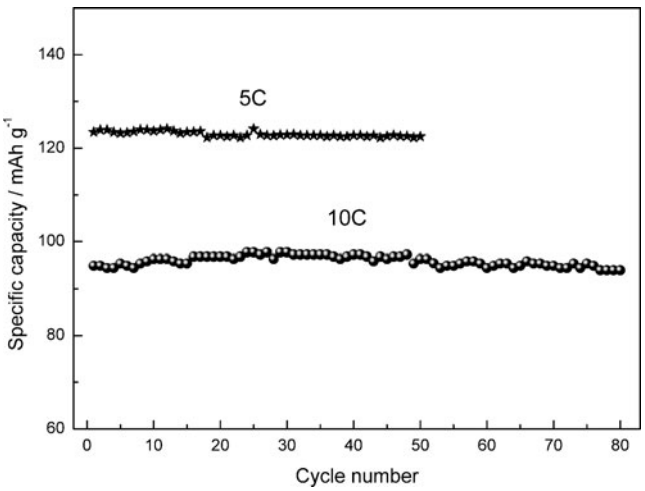

Fig. 12 Cycling performance of the $LiFePO_4$/C composite derived from optimized synthesis conditions

temperature and mole ratio of $Li_2C_2O_4$ to PAALi are investigated. The results certify that the synthesis temperature can obviously affect the particle size and crystallinity of $LiFePO_4$ and finally play an essential role in the electrochemical performance. Meanwhile, an appropriate mole ratio (carbon content) can lead to the most homogeneous particle size, highest conductivity, and smallest electrode polarization which are beneficial to the best electrochemical performance. With the optimized synthesis temperature at 700 °C and mole ratio of 1.17:1, the sample exhibits excellent rate performance and cycling stability.

References

1. Padhi AK, Nanjundaswamy KS, Goodenough JB (1997) J Electrochem Soc 144:1188
2. Ravet N, Chouinard Y, Magnan JF, Besner S, Gauthier M, Armand M (2001) J Power Sources 97:503
3. Islam MS, Driscoll DJ, Fisher CAJ, Slater PR (2005) Chem Mater 17:5085
4. Delacourt C, Poizot P, Levasseur S, Masquelier C (2006) Electrochem Solid-State Lett 9:A352
5. Wang L, Liang GC, Ou XQ, Zhi XK, Zhang JP, Cui JY (2009) J Power Sources 189:423
6. Kim CW, Lee MH, Jeong WT, Lee KS (2005) J Power Sources 146:534
7. Yu F, Zhang JJ, Yang YF, Song GZ (2009) Electrochim Acta 54:7389
8. Zhi X, Liang G, Wang L, Ou X, Gao L, Jie X (2010) J Alloys Compd 503:370
9. Zhang WK, Zhou XZ, Tao XY, Huang H, Gan YP, Wang CT (2010) Electrochim Acta 55:2592
10. Fey GTK, Chen YG, Kao HM (2009) J Power Sources 189:169
11. Zhi X, Liang G, Wang L, Ou X, Zhang J, Cui J (2009) J Power Sources 189:779
12. Liu H, Xie J, Wang K (2008) J Alloys Compd 459:521
13. Kim K, Cho YH, Kam D, Kim HS, Lee JW (2010) J Alloys Compd 504:166
14. Palomares V, Goñi A, Muro IGd, Meatza Ide, Bengoechea M, Cantero I, Rojo T (2010) J Power Sources 195:7661
15. Goktepe H, Sahan H, Kilic F, Patat S (2010) Ionics 16:203
16. Kimura M, Kolthoff IM, Meehan EJ (1973) J Phys Chem 77:1262
17. DeGraff BA, Cooper GD (1971) J Phys Chem 75:2897
18. Shi ZQ, Huang M, Huai YJ, Lin ZJ, Yang KR, Hu XB, Deng ZH (2011) Electrochim Acta 56:4263
19. Rodrigues S, Munichandraiah N, Shukla AK (1999) J Solid State Electrochem 3:397
20. Nobili F, Croce F, Scrosati B, Marassi R (2001) Chem Mater 13:1642